Density waves and jamming transition in cellular automaton models for traffic flow

1999 J. Phys. A: Math. Gen. 32 6517

(http://iopscience.iop.org/0305-4470/32/37/303)

J. Phys. A: Math. Gen. **32** (1999) 6517–6525. Printed in the UK PII: S0305-4470(99)04335-8

Density waves and jamming transition in cellular automaton models for traffic flow

L Neubert†, H Y Lee‡ and M Schreckenberg†

† FB 10, Theoretische Physik, Gerhard-Mercator-Universität Duisburg, 47048 Duisburg, Germany

‡ Department of Physics and Centre for Theoretical Physics, Seoul National University, Seoul 151-742, Korea

E-mail: neubert@traffic.uni-duisburg.de, schreck@traffic.uni-duisburg.de and agnes@phya.snu.ac.kr

Received 14 May 1999, in final form 2 July 1999

Abstract. In this paper computer simulation results of higher-order density correlations for cellular automaton models of traffic flow are presented. The examinations show the jamming transition as a function of both the density and the magnitude of noise and allow one to calculate the velocity of upstream moving jams. This velocity is independent of the density and decreases with growing noise. The point of maximum flow in the fundamental diagram determines its value. For that it is not necessary to explicitly define jams in the language of the selected model, but only based upon the well defined characteristic density profiles along the line.

1. Introduction

Recently, the examination and modelling of vehicular traffic has become an important subject of research—see [1–5] and references therein for a brief review. In the microscopic approach to the traffic flow problem, the cellular automaton introduced in [6] reproduces important entities of real traffic, like the flow–density relation or stop-and-go waves. Beside the realization of some basic requirements to such a model it can be efficiently used in computational investigations and applications [7–10]. Fundamental analytical and numerical examinations enclose exact solutions for certain limits and mean-field approximations [11]: the jamming transition [12–17] or the effects of perturbations and the occurrence of metastable states [18–20], for example.

We investigate the density waves and the separation in free-flow and dense regions by means of the density-autocorrelation function. It enables us to trace back the spatio-temporal evolution of jams which are stable during the measurement time, on condition that jams emerge. It should be noted that the probability for a jam to survive decreases with the simulation time [21] in a system without a clear phase separation between congestion and free flow. However, the duration of a simulation is sufficiently shorter than these time periods. By this method it is superfluous to give an explicit definition of what a jam is and which cars are belonging to the jam. Therefore, this method can be theoretically used for every traffic flow model where density profiles are available. As an example, we apply this method to cellular automaton models. In this context we report and discuss several aspects of the underlying model and their slow-to-start modifications (section 2): the jamming transition shows up by

0305-4470/99/376517+09$30.00

varying both the global density ρ and the global noise p; the jam velocity can be derived directly from the density-autocorrelation function and is closely related to the global flow–density relation (section 3). It is not the goal of this paper to discuss the jamming transition with regard to the criticality or the sharpness of this issue, but we apply the correlation function method from a more practical point of view.

2. The model

Within the framework of this paper we only consider a one-dimensional ring of cells. The cells are either vacant or occupied by a vehicle labelled i. Its position is x_i and its discrete velocity is $v_i \in [0, v_{max}]$. The gap g_i denotes the number of empty sites to its leading vehicle. The rules for a parallel update are:

- Acceleration with regard to the vehicle ahead: $v_i' \leftarrow \min(v_i + 1, g_i, v_{max})$,
- Noise: with a probability p do $v_i'' \leftarrow \max(v_i' - 1, 0)$,
- Movement: $x_i \leftarrow x_i + v_i''$.

The investigated systems consist of L cells and N vehicles, the global density is $\rho = N/L$. The flow is defined as $J = \langle v \rangle \rho$ with the mean velocity $\langle v \rangle = \sum v_i/N$. In the following the Nagel–Schreckenberg cellular automaton model [6] defined through the above set of rules is denoted by SCA.

We extend our studies on further modifications of the SCA, namely on models with slow-to-start rules. For the model with velocity-dependant randomization (VDR) [19, 20] we set $\tilde{p}(v_i = 0) = \mathrm{Min}(p + p_{VDR}, 1)$. This leads to a reduced outflow from a jam. Note that v_i is the velocity before the first update step is performed. The other modified model under consideration is the T^2 model introduced by Takayasu and Takayasu [22]. Here the headway, g_i, of a vehicle i controls the acceleration: standing vehicles with a headway $g_i = 1$ only speed up with a probability $1 - \tilde{p}$ with $\tilde{p} = \mathrm{Min}(p + p_{T^2}, 1)$, whereas for all others the rules are unchanged. Unlike the SCA with similar parameters, both models exhibit a different behaviour in the vicinity of the point of maximum flow ($\rho_{max} \equiv \rho(J_{max})$, J_{max}). They are capable of generating metastable states in the adiabatic approach (for details see [20]), i.e. one finds two branches of $J(\rho)$ in a small density interval. Additionally, for sufficiently small p one can find a clear separation of the dense and free-flow regions in a space-time plot. We summarize the effective deceleration probabilities of the applied models:

$$\begin{aligned}
&\text{SCA:} && p = \text{const.} \\
&\text{VDR:} && \tilde{p} = \begin{cases} \mathrm{Min}(p + p_{VDR}, 1) & v_i = 0 \\ p & \text{otherwise} \end{cases} \\
&\text{T}^2\text{:} && \tilde{p} = \begin{cases} \mathrm{Min}(p + p_{T^2}, 1) & v_i = 0 \wedge g_i = 1 \\ p & \text{otherwise.} \end{cases}
\end{aligned} \tag{1}$$

Actually, other definitions of $\tilde{p}$ are conceivable, but, for our purpose, we decided to only use the above notations. Primarily, it was done for modelling moving vehicles with similar properties and to scan the parameter space by only varying p. Both p_{VDR} and p_{T^2} are of any value, but fixed.

3. Simulation results and their discussion

The density waves are moving upstream and can be easily observed in a space-time plot [6, 23]: one finds separation of the dense and free-flow regions. For the measurements it is necessary

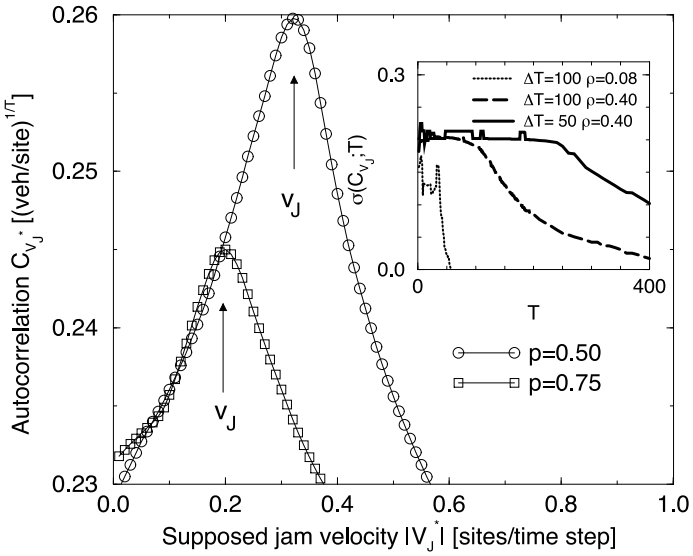

Figure 1. The peak of the density-autocorrelation function enables one to estimate the jam velocity, V_J. The standard deviation of the symmetrically assumed C_{V_J} is depicted in the inset. For large $T/\Delta T$ ratios the variance shrinks a lot, therefore it might occur that the autocorrelation function vanishes and inhibits the estimation of the dependant quantities. In the vicinity of ρ^* this sensitivity is more pronounced ($\rho = 0.4$).

to introduce the mean local density $\rho_l(k,t)$ of the cell k at time t:

$$\rho_l(k,t) = \frac{1}{\lambda}\sum_{i=0}^{\lambda-1}\eta_{k+i}(t) \tag{2}$$

with

$$\eta_{k+i}(t) = \begin{cases} 1 & \text{if site } k+i \text{ is occupied at time } t \\ 0 & \text{otherwise.} \end{cases}$$

The parameter λ denotes the length of the interval on which the local density has to be computed. It should satisfy the condition $\lambda_0 \ll \lambda \ll L$ [15] with a characteristic length scale λ_0. For the determination of the jam velocity, V_J, we use the generalized T-point autocorrelation function of the density

$$C_{V_J^*}(r \equiv V_J^*\tau\Delta T, \tau) = \left\langle \prod_{\tau=0}^{T-1} \rho_l(x + V_J^*\tau\Delta T, t + \tau\Delta T) \right\rangle_L \tag{3}$$

with the supposed jam velocity $V_J^* \in [-1, 0]$. By varying V_J^* one finds the largest $C_{V_J^*}(r,\tau)$ (figure 1). ΔT is the time interval between two single measurements which contributes to (3). Sufficiently large values of ΔT are necessary to observe a macroscopic motion and to determine V_J with adequate accuracy. Unless otherwise mentioned, we set $L = 10^4$ and $\Delta T = 10^2$ in order to exclude any finite-size effects. Usually, we average over 20 simulation runs with $v_{max} = 5$ and $\lambda = 30$.

As pointed out in figure 1, one has to thoroughly adjust the parameters T and ΔT. If T is of the order of magnitude of ΔT then the uncertainty of the measurement covers the signal of interest and C_{V_J} vanishes. This problem becomes more serious while approaching ρ^*. In this region the calculations are additionally complicated due to large fluctuations of C_{V_J} itself.

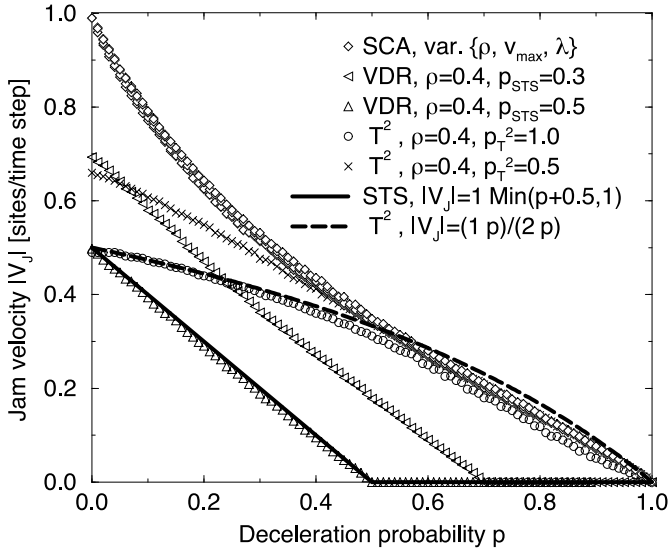

Figure 2. The jam velocity as a function of p, the error bars are within the symbol size ($\rho = 0.4$).

The jam velocity V_J depends on the deceleration probability p (figure 2) and is related to global quantities as shown later. We checked this for a variety of parameters, but could not notice any remarkable deviations among the diverse sets of data. The modifications of the SCA, VDR and T^2, yield a different behaviour. The absolute values of the jam velocity in the VDR and T^2 models are smaller than that of the SCA, implying that both modifications are characterized by a lowered outflow from a jam that, in turn, reduces the jam velocity.

The results of simulations using the VDR are basically shifted towards smaller $|V_J|$. p_{VDR} can be recognized on the ordinate at $p = 0$ and on the abscissa at $V_J = 0$, for large p a total deadlock occurs, i.e. it is highly unlikely or even impossible that a stopped car speeds up again. In order to find out how V_J is related to $\tilde{p}$ we investigate the mean waiting time t_w for $\tilde{p} < 1$ expressed through an infinite series:

$$t_w = 1(1-\tilde{p}) + 2(1-\tilde{p})\tilde{p} + 3(1-\tilde{p})\tilde{p}^2 \ldots = (1-\tilde{p})\sum_{n=1}^{\infty} n\tilde{p}^{n-1} = \frac{1}{1-\tilde{p}}$$
$$\Rightarrow |V_J| = \frac{1}{t_w} = 1 - \tilde{p} \in [0, 1 - p_{VDR}] \tag{4}$$

and is exact for $p = 0$. For large values of p_{VDR} one obtains a good agreement, whereas for small p_{VDR} the jam velocity is overestimated. This is due to the so-called sub-jams which emerge downstream from wider jams and cause a reduction of $|V_J|$.

The results drawn from simulations using the T^2 model show no deadlock situation for any $p < 1$. Starting with $p = 1$, one can hardly distinguish between the simulation results of SCA and T^2. This is especially valid as long as $p_{T^2} > 1 - p$. Similar to (4) one can estimate

$$\begin{aligned} t_w &= 1(1-\tilde{p}) + 2(1-p)\tilde{p} + 3(1-p)\tilde{p}p + 4(1-p)\tilde{p}p^2 \ldots \\ &= 1 + \tilde{p}\sum_{n=0}^{\infty} p^n = \frac{1-p+\tilde{p}}{1-p}. \end{aligned} \tag{5}$$

Note that for small p_{T^2}-values V_J is overestimated for all values of p, which, in turn, can be traced back to the occurrence of sub-jams. With increasing p_{T^2} even for small p it is required

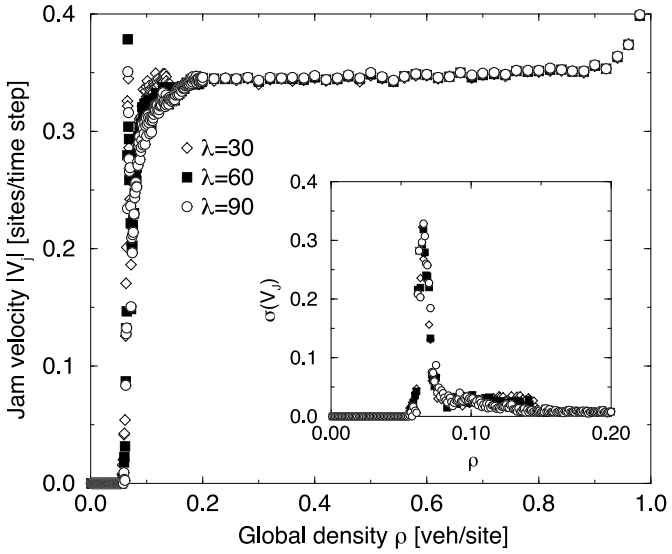

Figure 3. V_J versus ρ for $p = 0.5$. Beyond ρ^*, especially for $0.2 \leqslant \rho \leqslant 0.8$, $V_J(\rho)$ can be assumed to be constant. The inset reveals the large fluctuations of V_J near ρ^* which are up to the order of magnitude of V_J itself.

to set $\tilde{p} = 1$. Again, $|V_J| = t_w^{-1}$ and two special cases can be described by

$$|V_J|(p = 0) = \frac{1}{1 + p_{T^2}} \qquad \text{and} \qquad |V_J|(p_{T^2} \to 1) = \frac{1 - p}{2 - p}. \tag{6}$$

Obviously, the measurements reveals several density regimes. Below ρ^* the vehicles move independently, i.e. there are no correlations between them. For $\rho \geqslant \rho^*$ upstream-moving density waves can be detected by means of (3). In the vicinity of ρ^* the jam velocity reveals large fluctuations (figure 3), which are due to the recurrent emergence and dissipation of jams. But beyond ρ^*, V_J is nearly constant. Within the interval where density waves are to be expected it is obvious that V_J is independent of ρ, since the outflow from a jam is independent of the global density.

So far, we have applied the autocorrelation function (3) to determine the jam velocity. But this quantity itself indicates the two different phases separated by noise p^* or density ρ^* (figures 4 and 5). Varying p leads to a transition while crossing p^*. Its clarity strongly depends on $T/\Delta T$: for insufficient ratios a plateau at $\bar{C}_{V_J}(p)$ occurs. To elucidate it we used a modified autocorrelation

$$\bar{C}_{V_J^*}(r, \tau) = \left\langle \left(\prod_{\tau=0}^{T-1} \rho_l(x + V_J^* \tau \Delta T, t + \tau \Delta T) \right)^{1/T} \right\rangle_L. \tag{7}$$

The other transition takes place while crossing the density ρ^* (figure 5). For $\rho < \rho^*$ one finds empty regions on the road of the order of magnitude of λ, and therefore C_{V_J} completely vanishes. On the other hand, for $\rho > \rho^*$ stable congestion emerges. The same jam can be detected at t_i as well as at $t_f = t_i + \tau \Delta T$ located at $x(t_i) - |V_J| t_f$. In this context, ρ^* can be denoted as the density, at which stable jams emerge and separates the density regime as is shown in the inset of figure 5. For a fixed density and a varying v_{max} (figure 6) the relationship can be estimated as $C_{V_J}(v_{max}) \propto \rho$. Nevertheless, the quality of these data does not allow a correct classification of the transition between the free-flow and the dense region. Above all,

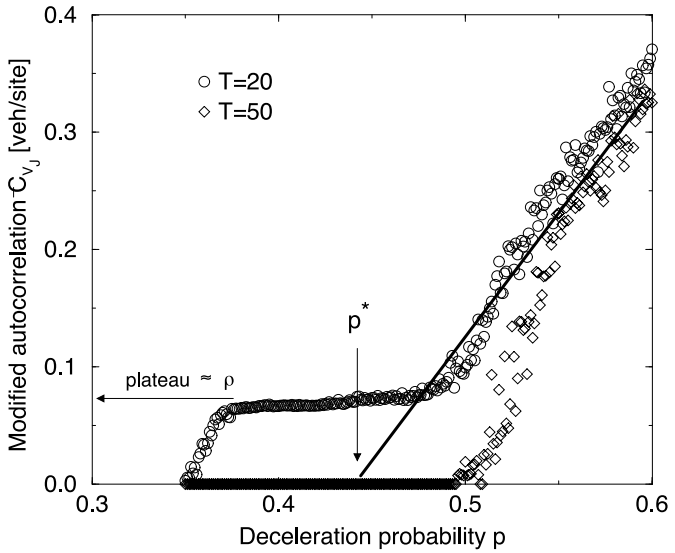

Figure 4. The transition from free flow to congested flow can also be obtained in the behaviour of the modified autocorrelation function $\bar{C}_{V_J}$ (7) by varying p ($\rho = 0.073$). The transition is smeared out due to finite-size effects and systematic errors in the determination of $\bar{C}_{V_J}$.

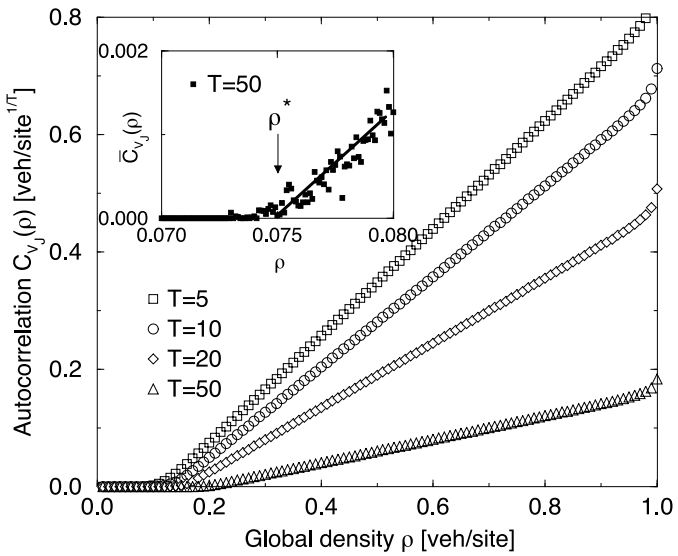

Figure 5. Plot of the the autocorrelation function $C_{V_J}(\rho)|_{v_{max}}$. Below a signified density the autocorrelation function vanishes due to the absence of jams. The inset zooms in on the region $\rho \approx \rho^*$ for the modified autocorrelation $\bar{C}_{V_J}$ (7) ($p = 0.5$).

the sensitive dependences on the many adjustable parameters of this method seem to prevent a more accurate consideration of the interesting interval of density.

How is the jam velocity related to other macroscopic quantities? In the steady state the dynamics are characterized by an equilibrium of out-flowing vehicles and vehicles attaching to the jam from behind. The more frequently vehicles join the jam, the faster the jam moves

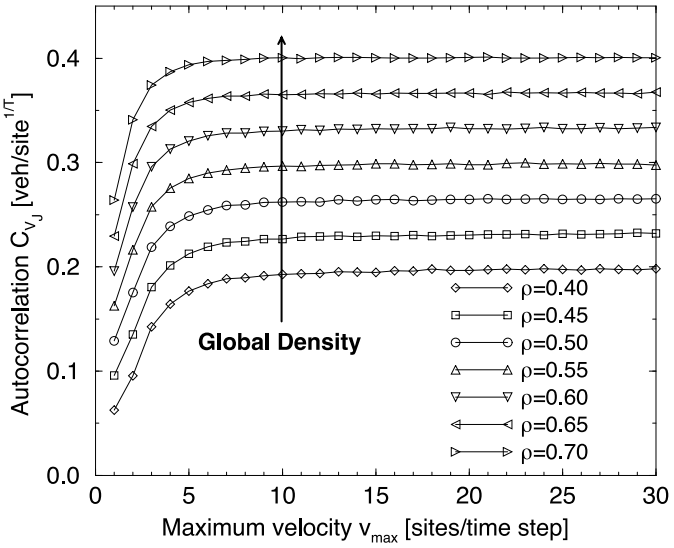

Figure 6. Plot of the the autocorrelation function $C_{V_J}(v_{max})|_\rho$ ($p = 0.5$).

upstream. If we neglect any effects due to metastability then the free-flow region can be assumed to be located in the vicinity of the point of maximum flow (ρ_{max}, J_{max}). Hence, the velocity of attaching vehicles is $\langle v_{att}\rangle = J_{max}/\rho_{max}$. The mean distance between the upstream tail of the jam and the next vehicle is $\langle g\rangle = \rho_{max}^{-1} - 1$ and the temporal distance therefore reads

$$\Delta t_{att} = \frac{\langle g\rangle}{\langle v_{att}\rangle} \Leftrightarrow V_J = \frac{J_{max}}{\rho_{max} - 1} \leqslant 0. \tag{8}$$

This is confirmed by the simulation results depicted in figure 7. It means that V_J is determined by the slope of the congested branch ($\rho \geqslant \rho_{max}$) in the fundamental diagram. This can also be verified for the VDR and T^2 modifications (figure 8). The small deviations from the data rest upon a difference between the outflow of the jam and the maximum global flow in the considered systems, but also in the above-made assumption of the equilibrium. Actually, the lowered outflow from jams observed in the VDR and T^2 models in comparison with the SCA is also reflected by (8).

Concluding, this knowledge enables a calibration of the SCA. Besides the approach of the fundamental diagram derived from empirical data, a further point of interest is the velocity of upstream-moving jams (≈ -15 km h^{-1} on German highways [24])—but according to (8) all the information is accumulated in the fundamental diagram, namely in the second characteristic slope of $J(\rho)$. For the SCA one can set $v_{max} = 5$ and $p = 0.2$–0.3 to adapt the simulation to this empirical jam velocity.

4. Summary

We have investigated the cellular automaton model for vehicular traffic in order to get information about the density waves and their velocity. Beside the standard SCA we also included two slow-to-start modifications (VDR and T^2). Both resemble the SCA except the rules for standing vehicles. Loosely speaking, they result in a lower flow downstream from a jam and a clear phase separation for certain density regimes. For the determination of the jam velocity we used the density-autocorrelation function $C_{V_J}(r, \tau)$. Despite the high

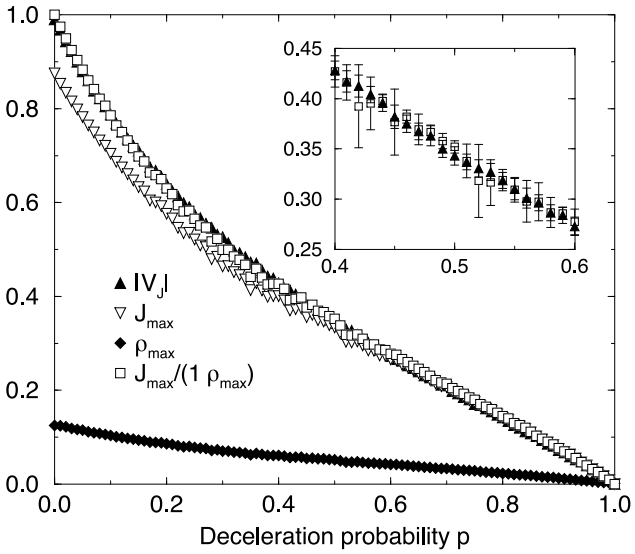

Figure 7. The jam velocity can be explained by (8): $V_J = J_{max}/(\rho_{max} - 1)$.

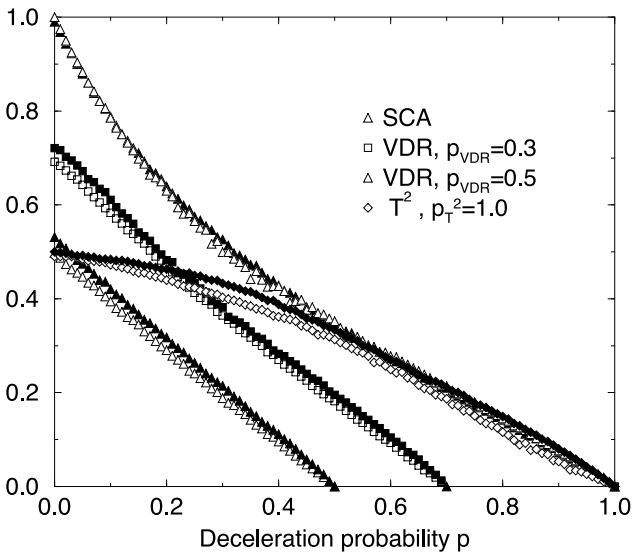

Figure 8. V_J (full symbols) as well as $J_{max}/(\rho_{max} - 1)$ (open symbols) are depicted for all models used. The small deviations are related to the discrepancies between the outflow of a jam and the global maximum flow.

computational efforts ($\mathcal{O}(L^2)$) this method was suitable for application to our calculations. Moreover, a definition of jams is not necessary and, therefore, the method can be applied to every model that provides density profiles along the road.

The quantity $C_{V_J}(r, \tau)$ reflects the two different phases and depends on the global density ρ. The density regime is separated by ρ^*. For $\rho < \rho^*$ no jams can be detected by the applied method, whereas for larger ρ the system is dominated by sequences of dense and free-flow regions, where C_{V_J} remains finite and permits one to estimate ρ^*. At this point a transition to

the congested region takes place. Both the local length λ and the number of calculations, T, have a large influence on C_{V_J}. Further statements regarding the transition cannot be given due to the numerical insufficiencies and accuracy.

The jam velocity can be derived directly from $C_{V_J}(r, \tau)$. For sufficiently large ρ the absolute value of V_J is a continuous and descending function of p, but depends on the model considered. The differences between the models, especially for $p \to 0$ and $p \to 1$, could be explained by waiting-time arguments. The jam velocity is essentially expressed through ρ_{max} and J_{max}, irrespective of the model considered here.

Acknowledgment

The authors would like to thank A Schadschneider for helpful discussions and his important remarks on this manuscript.

References

[1] Wolf D E, Schreckenberg M and Bachem A (ed) 1996 *Traffic and Granular Flow* (Singapore: World Scientific)
Schreckenberg M and Wolf D E (ed) 1998 *Traffic and Granular Flow '97* (Singapore: Springer)
[2] Lighthill M J and Whitham G B 1955 *Proc. R. Soc.* A **229** 281
[3] Kerner B S and Konhäuser P 1993 *Phys. Rev.* E **48** 2335.
[4] Bando M, Hasebe K, Nakayama A, Shibata A and Sugiyama Y 1995 *Phys. Rev.* E **51** 1035
[5] Helbing D 1997 *Phys. Rev.* E **55** 3735
[6] Nagel K and Schreckenberg M 1992 *J. Physique* I **2** 2221
[7] Chopard B, Luthi P O and Queloz P A 1996 *J. Phys. A: Math. Gen.* **29** 2325
[8] Rickert M and Wagner P 1996 *Int. J. Mod. Phys.* C **7** 133
[9] Esser J and Schreckenberg M 1997 *Int. J. Mod. Phys.* C **8** 1025
[10] Esser J, Neubert L, Wahle J and Schreckenberg M 1999 *Proc. 14th Int. Symp. on Transportation and Traffic Theory (Jerusalem)* (Amsterdam: Pergamon)
[11] Schadschneider A and Schreckenberg M 1993 *J. Phys. A: Math. Gen.* **26** L679
Schadschneider A and Schreckenberg M 1997 *J. Phys. A: Math. Gen.* **30** L69
Schadschneider A and Schreckenberg M 1998 *J. Phys. A: Math. Gen.* **31** L225
[12] Csanyi G and Kertész J 1995 *J. Phys. A: Math. Gen.* **28** 427
[13] Sasvari M and Kertész J 1997 *Phys. Rev.* E **56** 4104
[14] Eisenblätter B, Santen L, Schadschneider A and Schreckenberg A 1998 *Phys. Rev.* E **57** 1309
[15] Lübeck S, Schreckenberg M and Usadel K D 1998 *Phys. Rev.* E **57** 1171
[16] Cheybani S, Kertész J and Schreckenberg M 1998 *J. Phys. A: Math. Gen.* **31** 9787
[17] Roters L, Lübeck S and Usadel K D 1999 *Phys. Rev.* E **59** 2672
[18] Krauß S, Wagner P and Gawron C 1997 *Phys. Rev.* E **55** 5597
[19] Schadschneider A and Schreckenberg M 1997 *Ann. Phys.* **6** 541
[20] Barlovic R, Santen L, Schadschneider A and Schreckenberg M 1998 *Eur. Phys. J.* B **5** 793
[21] Nagel K 1994 *Int. J. Mod. Phys.* C **5** 567
[22] Takayasu M and Takayasu H 1993 *Fractals* **1** 860
[23] Treiterer J and Myers J A 1974 *Proc. 8th Int. Symp. on Transportation and Traffic Theory* (Sydney: Reed)
[24] Kerner B S and Rehborn H. *Phys. Rev.* E **53** R1297